

# Failure Assessment Curve of Orthotropic TA2 Pipe with Circumferential Through-wall Crack

Qu Wenjun, Zhou Changyu, Yu Qin

Nanjing Tech University, Nanjing 211816, China

**Abstract:** The limit loads,  $J$  integral results and failure assessment curve (FAC) of the circumferential through-wall cracked isotropic and orthotropic pipes of pure titanium TA2 were calculated based on the 3-dimensional (3-D) elastic-plastic finite element (FE) analyses. The effects of pipe geometry, crack size and orthotropy on the FAC were investigated. Calculation results show that the limit load and  $J$  integral of the isotropic pipe and the anisotropic pipe are obviously different. For the failure assessment curves, when the load ratio  $L_r < 0.9$ , if the orthotropic material is evaluated as an isotropic material, the evaluation result is conservative. On the contrary, when the load ratio  $L_r > 0.9$  and if the orthotropic material is evaluated as an isotropic material, the evaluation result is somewhat dangerous. And it is most dangerous when the mechanical properties of the orthotropic material in axial direction are stronger than in circumferential direction. Thus the orthotropy of circumferential through-wall crack pipe cannot be neglected for defect assessment.

**Key words:** TA2; orthotropy; limit load;  $J$  integral; failure assessment curve; circumferential through-wall cracked pipe

Titanium and its alloys have many advantages such as good heat resistance, good corrosion resistance and high strength<sup>[1]</sup>. As a new type of structural material with broad development prospects, titanium is used more and more extensively. Since titanium tube is put on the market, it has become a preferred material for condenser and heat exchanger<sup>[2]</sup>. With the extensive application of titanium, the problem of safe use of pressurized titanium structures has also attracted increasing attention. Among the structural defects, the pipe crack is very common.

For the safe operation and efficient maintenance of piping components in plants, a reliable defect assessment method is necessary. Based on the fracture mechanics theory, the structural integrity safety evaluation system was established according to the fitness for service, which has been widely used all over the world<sup>[3, 4]</sup>. In order to establish the failure assessment curves of cracked pipes, the determination of  $J$ -integral and limit load of cracked pipes is essential. For instance, Kumar<sup>[5]</sup> et al introduced plastic influence functions for  $J$  of pipes with a circumferential through-wall crack (TWC). Zahoor<sup>[6]</sup> extended the applicability of the solutions to

axial and circumferential TWC. Park<sup>[7]</sup> et al investigated the plastic influence functions for the thin-walled pipes with a circumferential TWC. Extensive investigations<sup>[8,9]</sup> have been made to determine limit loads of cracked pipes under various loading conditions. Furthermore, the failure assessment curve of TA2 was studied by Chen et al<sup>[10]</sup>. The failure assessment curves of titanium pipes containing surface cracks under room temperature creep have been studied by Dai et al<sup>[11]</sup>. However, the orthotropy of alloy is seldom considered in the researches listed above. Generally, titanium is regarded as an isotropic material in engineering applications, while many experiments have proved that titanium is orthotropic<sup>[12]</sup>, and the pipes also show orthotropy in the circumferential, radial and axial directions. It was found that the difference between the circumferential direction and the axial direction has an influence on the crack propagation<sup>[13]</sup>. If the titanium is treated as an isotropic material in the defect assessment, the result may be inaccurate. Bai et al<sup>[14]</sup> has studied the failure assessment curves of orthotropic central crack specimen and proved the necessity of considering the effect of orthotropy on the FAC. Therefore, it is very meaningful to study the safety

Received date: April 26, 2018

Foundation item: National Natural Science Foundation of China (51475223, 51675260)

Corresponding author: Zhou Changyu, Ph. D., Professor, School of Mechanical and Power Engineering, Nanjing Tech University, Nanjing 211816, P. R. China, Tel: 0086-25-58139951, E-mail: changyu\_zhou@163.com

Copyright © 2019, Northwest Institute for Nonferrous Metal Research. Published by Science Press. All rights reserved.

assessment of orthotropic titanium pipe containing through-wall cracks.

In the present paper, in order to obtain failure assessment curves of orthotropic titanium pipe with circumferential through-wall crack, three-dimensional finite element (FE) analyses for circumferential through-wall cracked pipe were performed. In terms of the effects of orthotropy, both isotropic and orthotropic pipes were considered with different crack angles and ratios of pipe mean radius to thickness.

### 1 Finite Element Analysis

#### 1.1 Material properties

Many experiments have shown that there are obvious differences in the mechanical properties between circumferential and axial directions of the titanium pipe. Some have proved that the mechanical properties in circumferential direction are stronger than those in axial direction<sup>[12]</sup>. However, the material parameters of different batches will fluctuate due to the differences in chemical composition and molding process. Ref.[15] demonstrates two opposite results, that is, the material parameters in axial direction are greater or lower than those in circumferential direction for aluminum pipe. In order to consider the effect of circumferential and axial mechanical parameters on failure assessment curves, a finite element model was created under four conditions in the present work. "Isotropy 1" pipe takes the material parameters of set 1 which is of isotropy with lower strength. "Isotropy 2" pipe takes the material parameters of set 2 which is of isotropy with higher strength. "Orthotropy1" pipe takes set 1-2, and "orthotropy 2" pipe takes set 2-1. Set 1-2 means that the properties of axial direction take set 1, and the properties of circumferential direction take set 2. Set 2-1 means the opposite definition. The data of mechanical properties are shown in Table1. As shown in Fig.1, when the material parameters of orthotropy in circumferential direction are greater than those in axial direction, it is defined as "orthotropy 1". Otherwise, it is defined as "orthotropy 2".

For isotropic material, the Ramberg-Osgood stress-strain law is a fit table, and the stress-strain relationship is expressed as:

$$\frac{\epsilon}{\epsilon_y} = \frac{\sigma}{\sigma_y} + \alpha \left( \frac{\sigma}{\sigma_y} \right)^n \tag{1}$$

where  $\sigma_y$ ,  $\epsilon_y$ ,  $\alpha$  and  $n$  denote the yield strength, strain at yield strength, coefficient of R-O idealization and strain hardening exponent, respectively. According to the tensile test, the stress-strain relationship is obtained, and the material parameters  $\alpha$  and the hardening exponent  $n$  are also obtained. The results are seen in Table1.

For orthotropic pipe, it has nine independent elastic constants in three orthotropic directions, including three elastic modulus, 3 Poisson's ratios and 3 shear modulus. The properties of orthotropic materials are characterized by Hill yield criterion. As the wall thickness is thin, it is difficult to obtain the radial material parameters. In this paper, they are replaced by the average value of axial and circumferential properties<sup>[16]</sup>.

#### 1.2 Finite element model and boundary conditions

Fig.2 depicts a circumferential through-wall cracked pipe with relevant dimensions under internal pressure  $p$ . The mean radius and the thickness of pipe are denoted as  $R_m$  and  $t$ , respectively. The crack length is characterized by the half crack angle  $\theta$ . To quantify the effect of pipe geometry and crack size on failure assessment, three different values of  $R_m/t$  were employed,  $R_m/t=5, 10, 20$ , and three different values of  $\theta$  were considered,  $15^\circ, 30^\circ$  and  $45^\circ$ .

The FE models of titanium pipe with circumferential through-wall crack were built with the number of elements ranging from 962 to 1324. Symmetry conditions were used in the FE models to reduce the computing time, and only one quarter of the pipe was modeled. The length of the pipe is three times longer than the diameter which is long enough to eliminate the effect of boundary condition. Fig.3 depicts the FE mesh for  $R_m/t=5$  and  $\theta=30^\circ$ , and a ring of wedge-shaped elements was used in the crack-tip region. The crack tip mesh is

Table 1 Mechanical properties of TA2

Set	Elastic modulus/GPa	Yield strength/MPa	Poisson's ratio, $\nu$	Material parameters, $\alpha$	Hardening exponent, $n$
1	102	284	0.34	0.816	10.54
2	122	308	0.34	1.22	12.81

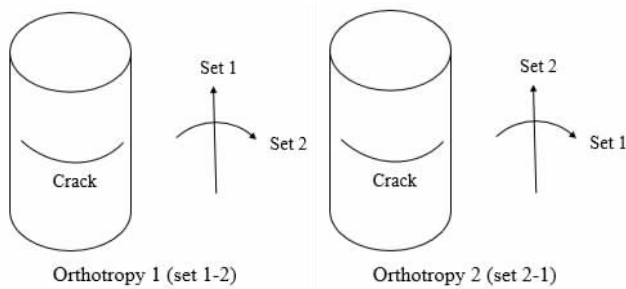


Fig.1 Two different orthotropic cases

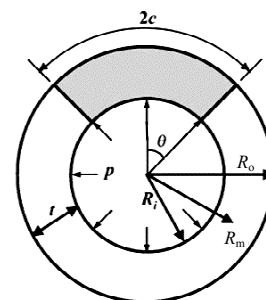


Fig.2 Schematic illustration of TWC pipes

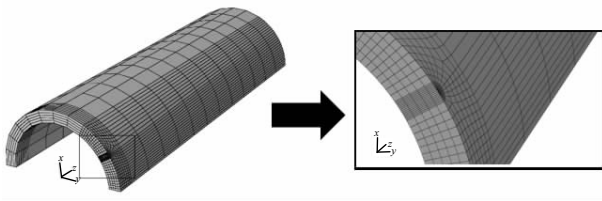


Fig.3 Typical finite element meshes of circumferential through-wall cracked pipe with  $R_m/t=5$  and  $\theta=30^\circ$

refined and the minimum size of crack tip mesh is 0.034 mm. To avoid problems associated with incompressibility, reduced integration elements (element type C3D8R in ABAQUS) were used. In order to calculate FE  $J$  integral, a total of 5 contours were considered around crack-tip. In addition to the first contour, the results of the 2nd to 5th contour were basically the same, the maximum error was less than 1% of each contour, and the 2nd to 5th contour were used for  $J$  integral calculations by averaging<sup>[17]</sup>.

Internal pressure was applied as a distributed load on the inner surface of FE model, together with an equivalent axial stress. More importantly, to consider the effect of crack face pressure, 50% internal pressure was applied to the crack face in the present work<sup>[18]</sup>.

## 2 Analysis of $J$ Integral and Plastic Limit Load According to Finite Element Results

### 2.1 Limit load for isotropic and orthotropic pipes with circumferential through-wall crack

The effect of plasticity on failure assessment diagram is expressed in abscissa  $L_r$ , which is defined as the ratio of applied load to limit load of the structure,  $P/P_0$ . In finite element calculation, based on the calculated load-displacement curve, the limit load  $P_0$  of the structure can be determined according to the twice elastic slope criterion<sup>[19]</sup>.

The limit loads of circumferential through-wall cracked isotropic and orthotropic pipes are shown in Fig.4a~4c. Generally, the limit load of circumferential through-wall

cracked pipe is inversely proportional to the crack angle and ratios of pipe mean radius to thickness for both orthotropic pipe and isotropic pipe. It is obvious that the limit load of orthotropic pipe is greater than that of isotropic pipe. The orthotropy of pipe material has a certain influence on the loading capacity of the pipe. If titanium is regarded as an isotropic material in the defect assessment, there is a certain error, so the effect of orthotropy on limit load cannot be neglected.

As we can see in Fig.4, with the change of angle, the difference between the limit load of orthotropic pipe and isotropic pipe is basically unchanged or slightly reduced, and the limit load of "orthotropy 1" pipe is always 2%~6% greater than that of "orthotropy 2" pipe. The difference remains basically stable with the increase in crack size. This indicates that the difference in mechanical properties between the circumferential and axial direction of titanium pipes affects the limit load of orthotropic pipe.

Ref.[14] has studied above two different cases of orthotropic central crack specimen. The results show that the limit loads, when the crack propagation direction is perpendicular to the rolling direction (same as set 1-2), are greater than those when the crack propagation direction is consistent with the rolling direction (same as set 2-1). Similarly, in the present paper, the limit pressures of "orthotropy 1" pipe are greater than those of "orthotropy 2" pipe.

### 2.2 $J$ integral calculation of circumferential through-wall cracked pipe

$J$  integral is related to the ordinate  $K_I r$ , which is defined as the square root of elastic integral and elastic-plastic integral ratio. It is also one of the important contents of the FAC.

#### 2.2.1 Influence of orthotropy on circumferential through-wall cracked pipe

In order to study the effect of orthotropy on the  $J$  integral results, the orthotropic results are compared with the isotropic results under different crack angles and different ratios of pipe mean radius to thickness. Fig.5 shows the  $J$  integral curve of the circumferential through-wall cracked orthotropic TA2 pipe.

As shown in Fig.5a~5c, in general, there is a big difference

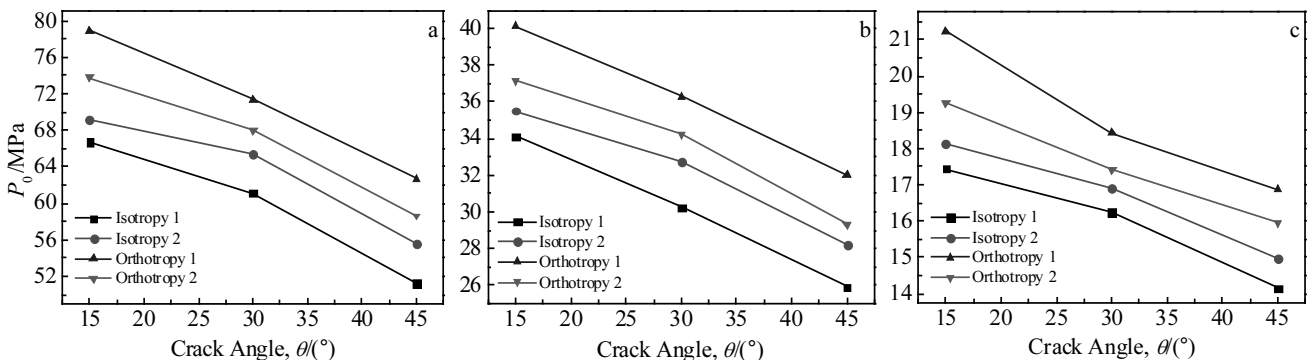


Fig.4 Limit loads of circumferential through-wall cracked TA2 pipe: (a)  $R_m/t=5$ , (b)  $R_m/t=10$ , and (c)  $R_m/t=20$

of  $J$  integral between isotropic pipe and orthotropic pipe, and the difference is bigger as the crack angle decreases. And as shown in Fig.5a, 5d and 5e, the thicker the wall thickness of pipe, the greater the effect of orthotropy on  $J$  integral. Under a lower internal pressure, the difference between orthotropic results and isotropic results is very small. As can be known from the previous section, the limit load of orthotropic pipe is greater than that of isotropic pipe. When the load reaches the limit load of the pipe, a wide range of yield phenomenon will appear in the crack tip, and the pipe is in the plastic deformation stage, resulting in a significant increase in  $J$  value. So with the increase of internal pressure, the  $J$  integral of circumferential through-wall cracked isotropic pipe increases significantly earlier than that of the orthotropic pipe, and so does the increasing rate. Compared to orthotropic pipes, isotropic cracked pipes will crack first.

Similarly, the limit loads of “orthotropy 2” pipe are less than those of “orthotropy 1” pipe, so the  $J$  integral of “orthotropy 2” pipe presents a significant increase first. And the  $J$  integral increasing rate of “orthotropy 2” pipe is greater than that of “orthotropy 1” pipe. After the significant increase appears, the  $J$  integral of “orthotropy 1” pipe is obviously smaller than in other cases, indicating that crack propagation is relatively not easy to occur.

In conclusion, the orthotropy has a great influence on  $J$  integral. The difference of mechanical properties between the circumferential and the axial direction of the titanium pipes affects  $J$  integral.

### 2.2.2 Influence of crack size and load on $J$ integral

Since the change trends of  $J$  integral are similar under different ratios of pipe mean radius to thickness, taking  $R_m/t=5$  as an example, the effect of crack angle and load on  $J$  integral is demonstrated in Fig.6.

Fig.6b shows that the crack size has little effect on  $J$  integral at lower internal pressure. However, with the increase of crack angle, the difference in  $J$  integral at different crack angles is obvious. And the larger the crack angle, the more sensitive the  $J$  integral to the load, especially when the crack angle is greater than  $30^\circ$ . From the calculation of limit load, it is known that the limit load decreases almost linearly as the crack angle increases. When the load reaches the limit load of the pipe, a wide range of yield phenomenon will appear in the crack tip, and the pipe is in the plastic deformation stage, resulting in a significant increase in  $J$  value. So as can be seen in Fig.6a, the larger the crack size, the faster the  $J$  integral increasing rate, and the smaller the loading capacity of the pipe.

### 2.3 $J$ integral and plastic limit load based on EPRI method

#### 2.3.1 Original EPRI method for circumferential through-wall crack

The EPRI method can provide  $J$  integrals using the plastic influence functions calibrated by FE analyses based on R-O relation for through-wall cracked pipes<sup>[5]</sup>. In this method, the  $J$  integral according to the applied load is calculated by summing elastic  $J$  and plastic  $J$ , as in following equation.

$$J = J_e(a) + J_p(a, n) \tag{2}$$

where  $J_e$  and  $J_p$  denote elastic and plastic  $J$  integral, respectively.

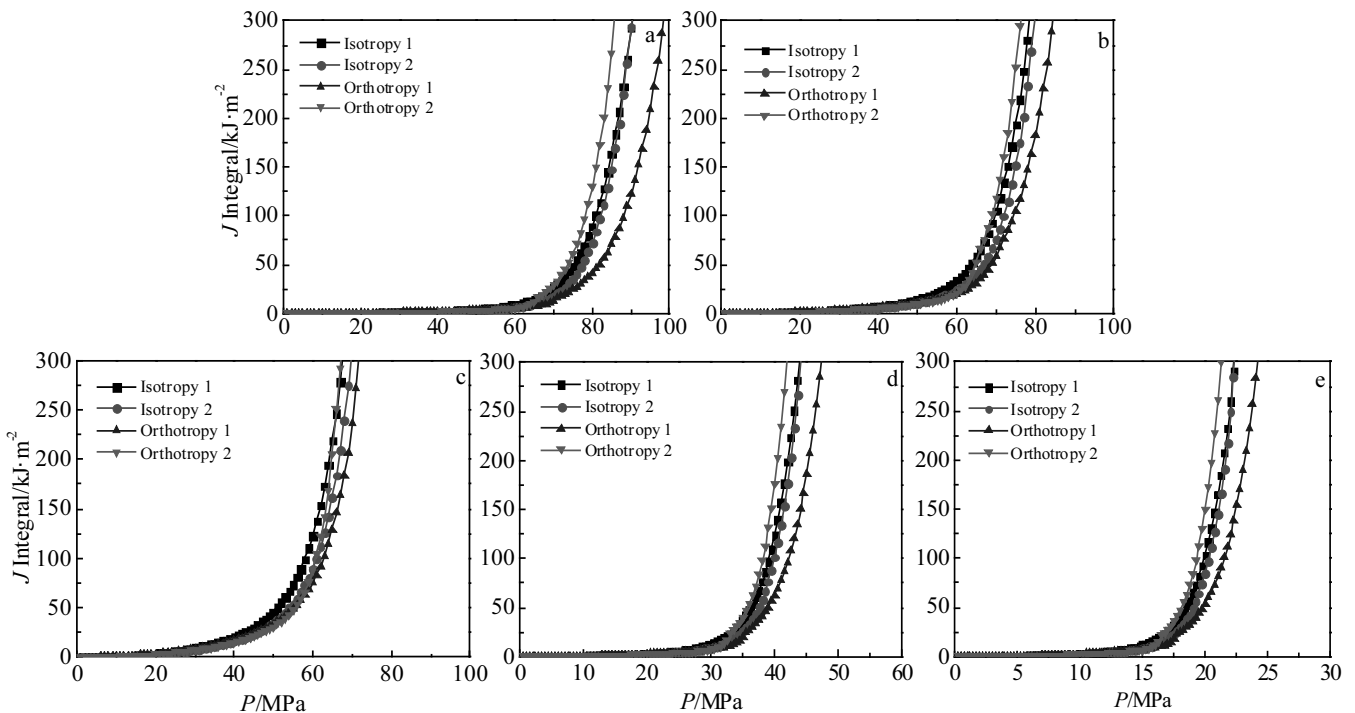


Fig.5  $J$  integrals of circumferential TWC pipe for orthotropic TA2: (a)  $R_m/t=5, \theta=15^\circ$ ; (b)  $R_m/t=5, \theta=30^\circ$ ; (c)  $R_m/t=5, \theta=45^\circ$ ; (d)  $R_m/t=10, \theta=15^\circ$ ; (e)  $R_m/t=20, \theta=15^\circ$

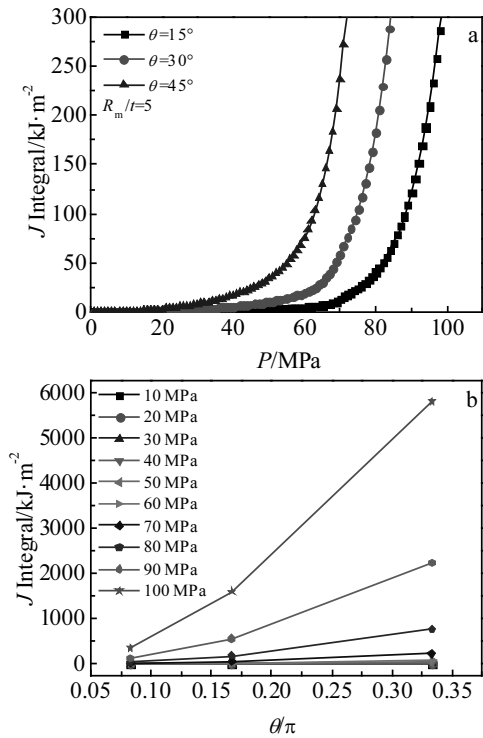


Fig.6 Influence of load (a) and crack angle (b) on  $J$  integral of "orthotropy 1" pipe

The elastic  $J$  integral for the circumferential through-wall cracked pipes can be expressed by following equation.

$$J_e = \frac{K_I^2}{E'} \quad (3)$$

where  $K_I$  denotes a remote stress intensity factor,  $E'=E$  for plane stress,  $E'=E/(1-\nu^2)$  for plane strain condition,  $E$  is elastic modulus of the material, and  $\nu$  is Poisson's ratio.

The plastic  $J$  for circumferential through-wall cracked pipes can be estimated by the related geometric variables, as in the following equation<sup>[20]</sup>.

$$J_p = \alpha \sigma_y \varepsilon_y R_m \frac{\theta}{\pi} (\pi - \theta) h_1 \left( \frac{R_m}{t}, \frac{\theta}{\pi}, n \right) \left( \frac{P}{P_0} \right)^{n+1} \quad (4)$$

where  $h_1$  denotes the plastic influence function for the  $J$  estimation.  $P$  denotes the magnitude of the applied load and  $P_0$  denotes the plastic limit load corresponding to the applied load. The  $\sigma_y$ ,  $\varepsilon_y$ ,  $\alpha$  and  $n$  denote the yield strength, strain at yield strength, coefficient of R-O idealization and strain hardening exponent, respectively.

### 2.3.2 Modified plastic influence function for circumferential through-wall cracked pipe

In order to calculate  $J$  integrals of circumferential through-wall cracked pipes based on EPRI method, the plastic influence functions for circumferential through-wall cracked pipes,  $h'_1$ , should be developed according to crack size, pipe geometries and strain hardening exponents of materials. The plastic  $J$  for calibration of plastic influence functions was

calculated by the FE  $J$  values as follows.

$$J_p = J_{FE} - J_e \quad (5)$$

where  $J_{FE}$  denotes the total  $J$  integral obtained from elastic-plastic FE analyses. Elastic  $J$  values are calculated from the elastic FE analyses for circumferential through-wall pipe. Rewriting Eq.(6) with respect to  $h'_1$ :

$$h'_1 = \frac{J_p}{\alpha \sigma_y \varepsilon_y R_m \frac{\theta}{\pi} (\pi - \theta) \left( \frac{P}{P_0} \right)^{n+1}} = \frac{J - J_e}{\alpha \sigma_y \varepsilon_y R_m \frac{\theta}{\pi} (\pi - \theta) \left( \frac{P}{P_0} \right)^{n+1}} \quad (6)$$

The plastic  $J$  integral and elastic-plastic  $J$  integral are taken into the Eq.(6) to obtain the change of coefficient with load. As shown in Fig.7, the value, when the load reaches the stability, is taken as the whole plastic solution coefficient. The new plastic influence functions for circumferential through-wall crack in pipe are presented in Table 2. Taking  $R_m/t=5$  and  $\theta=30^\circ$  as example, Fig.8 compares the FE  $J$  results with those using the proposed EPRI-based estimates. It can be seen that the modified EPRI-based  $J$  estimates are overall in good agreements with the FE results. The error between the two results is less than 2%.

### 2.3.3 Fitting of orthotropic limit loads for circumferential through-wall cracked pipe based on GE/EPRI method

Limit load formula of typical samples is given in the EPRI

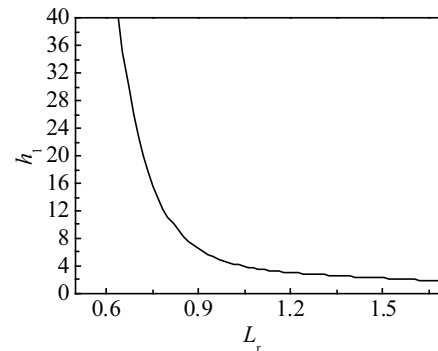


Fig.7 Variation of  $h_1$  with  $L_r$

Table 2 Plastic influence functions for circumferential TWC in pipe

Ratio of pipe mean radius to thickness	Pipe	$h'_1$		
		15°	30°	45°
$R_m/t=5$	Isotropy 1	2.58	1.91	0.58
	Isotropy 2	1.4	1.32	0.33
	Orthotropy 1	7	5.7	3.45
	Orthotropy 2	5.97	3.83	0.96
$R_m/t=10$	Isotropy 1	4.54	2.02	0.91
	Isotropy 2	2.78	1.56	0.54
	Orthotropy 1	12.9	8.92	6.13
	Orthotropy 2	9.19	4.6	1.18
$R_m/t=20$	Isotropy 1	4.75	3.47	1.93
	Isotropy 2	3.01	1.85	0.96
	Orthotropy 1	20.09	8.19	4.31
	Orthotropy 2	12.22	5.02	3.07

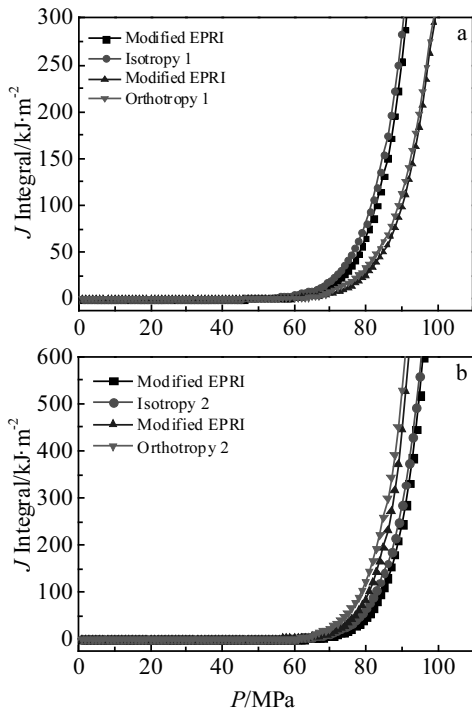


Fig.8 Comparison of the FE *J* results with those calculated using the modified GE/EPRI-based estimates: (a) isotropy 1 and orthotropy 1 and (b) isotropy 2 and orthotropy 2

engineering method. In these years, the scholars have performed a lot of analyses on the limit load for other structures or loading conditions and proposed corresponding analytical solutions.

In this section, for isotropic material, the calculated limit load is normalized, that is, the data is processed as the form  $P_0 R_m / 2\sigma_y t$ . The specific data of limit load are analyzed, and the relationship between the limit load and the crack size is considered as follows:

$$\frac{P_0 R_m}{2\sigma_y t} = f\left(\frac{\theta}{\pi}\right) \tag{7}$$

Based on FE results of  $R_m/t=5$ , the following polynomial approximation is proposed.

Isotropy 1:

$$\frac{P_0 R_m}{2\sigma_y t} = -2.738\left(\frac{\theta}{\pi}\right)^2 + 0.0951\left(\frac{\theta}{\pi}\right) + 0.5982 \tag{8}$$

Isotropy 2:

$$\frac{P_0 R_m}{2\sigma_y t} = -3.5532\left(\frac{\theta}{\pi}\right)^2 + 0.524\left(\frac{\theta}{\pi}\right) + 0.5419 \tag{9}$$

However, in order to obtain a simple engineering estimation method for the limit load of orthotropic pipe, orthotropic materials can be simplified to isotropic materials by introducing parameter *m* and making  $P_0' = m \cdot P_0$ . Eq.(10) and (11) are

obtained by the regression of the ratio of the orthotropic limit load and the isotropic limit load in FE result.

Orthotropy 1:

$$m = 5.1583\left(\frac{\theta}{\pi}\right)^2 - 1.4733\left(\frac{\theta}{\pi}\right) + 1.2700 \tag{10}$$

Orthotropy 2:

$$m = 3.0437\left(\frac{\theta}{\pi}\right)^2 - 1.0871\left(\frac{\theta}{\pi}\right) + 1.1372 \tag{11}$$

In order to verify the rationality of the fitting formula, the parameter *m* results of  $R_m/t=5, 10, 20$  and the proposed polynomial approximation are compared in Fig.9. The gap between the *m* results of  $R_m/t=5, 10, 20$  and the proposed polynomial approximation is all within 2%, which indicates that the fitting formula is reasonable.

### 3 Failure Assessment Curves

According to the limit load calculated in section 2.1 and the results of *J* integral, the FAC of the circumferential through-wall cracked pipe is obtained by R6 option 3.

The FAC of the isotropic and orthotropic pipes with circumferential through-wall crack is analyzed and compared in Fig.10. For the isotropic pipe, the failure assessment curves of “isotropy 1” pipe are slightly different from those of the “isotropy 2” pipe due to the material properties, but the overall trend is consistent. The FAC for the orthotropic pipe is slower than that for isotropic pipe when the load is relatively low ( $L_r < 0.8$ ), and it decreases rapidly when the load ratio reaches about 0.9. The failure assessment curves are also different in different orthotropic cases. When  $L_r < 0.9$ , the FAC of “orthotropy 1” pipe is located under the FAC of “orthotropy 2” pipe, and when  $L_r > 0.9$ , the opposite is true.

It can be seen from Fig.10 that four failure assessment curves have an intersection at a load ratio of about 0.9. When  $L_r < 0.9$ , as observed in Fig.10a~10c, the failure assessment

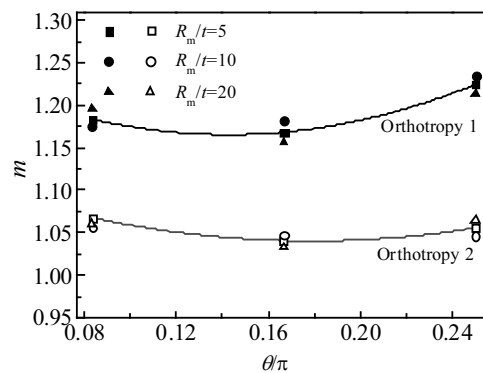


Fig.9 Comparisons of the parameter *m* results with the proposed polynomial approximation

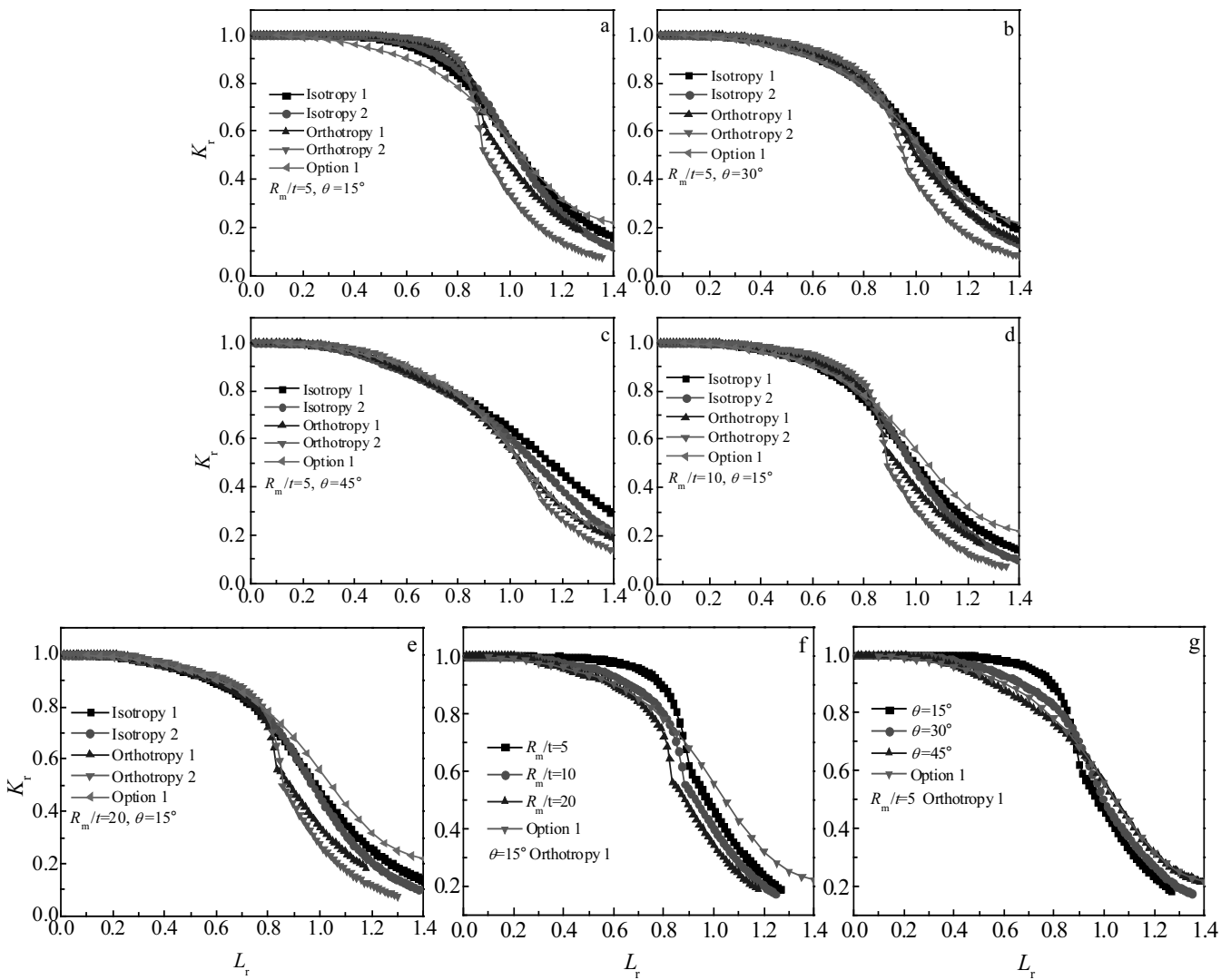


Fig.10 Failure assessment curves of isotropic and orthotropic TA2 pipe with circumferential TWC

curves of orthotropic pipes are located above the isotropic pipes. But the failure assessment curves of orthotropic pipes and isotropic pipes become closer and closer with the increase in crack angle, indicating that if the cracked titanium structure is evaluated as isotropy, the results will be conservative at lower loads and smaller crack angles. At the same time, according to Fig.10a, 10d and 10e, as the wall thickness of the pipe decreases, the failure assessment curves of orthotropic pipes and isotropic pipes gradually overlap.

When the load ratio is greater than 0.9, the failure assessment curves of orthotropic pipe are always located under the isotropic pipe, indicating that if the titanium is simplified as isotropic material, the evaluation results are somewhat dangerous. And as can be observed in Fig.10, the FAC of “orthotropy 2” pipe is always at the bottom when the load ratio is larger than 0.9, indicating that it is the most dangerous when the mechanical properties in the axial direction are stronger than those in

circumferential direction. So when the failure assessment of orthotropic structures with cracks is carried out, not only the orthotropic properties of the material but also the size of circumferential and the axial mechanical parameters should be considered.

As depicted in Fig.10a~10c, when  $L_r < 0.9$ , R6 option 1 can provide a safe but conservative failure assessment result when  $R_m/t = 5$ . According to Fig.10f, when  $R_m/t = 10, 20$ , the R6 option 1 is also safe. But with the increase of load, the R6 option 1 and R6 option 3 have an intersection, so the R6 option 3 is fitter for specific materials and structures. In addition, as we can see in Fig.10g, the intersection point moves backward with the increase of crack angle, which suggests that the application range of R6 option 1 decreases with increasing the angle.

#### 4 Conclusions

1) The limit load of orthotropic pipe is greater than that of

isotropic pipe. And the limit load of circumferential through-wall cracked orthotropic pipe is inversely proportional to the crack angle. Based on EPRI method, the calculated limit load is normalized, and then a formula for calculating the limit load is obtained.

2) The  $J$  integral of isotropic pipe is greatly different from that of orthotropic pipe. The difference in mechanical properties between the circumferential and axial direction of the titanium pipes affects  $J$  integral. And the larger the crack size, the faster the  $J$  integral growth rate. Based on the FE results, the new plastic influence functions for circumferential through-wall cracked pipe are proposed.

3) If the orthotropic material is evaluated as an isotropic material, the evaluation results are conservative when the load ratio  $L_r < 0.9$ . When the load ratio  $L_r > 0.9$ , the evaluation result is unsafe, and it is most dangerous when the mechanical properties in the axial direction are stronger than those in circumferential direction.

4) R6 option 1 is not fully safe for the failure assessment of orthotropic TA2 pipes with circumferential TWC. When the material parameters are known in different directions, the failure assessment curve of specific material and structure can be obtained by the finite element method using R6 option 3, which can be used as a basis for the evaluation of orthotropic TA2 pipes with circumferential TWC.

## References

- Zhao Yongqing. *Advanced Materials Industry*[J], 2007, 10: 28 (in Chinese)
- Jin Yu. *China Titanium Industry*[J], 2015, 4: 12 (in Chinese)
- Dowling A R, Townley C H A. *International Journal of Pressure Vessels and Piping*[J], 1975, 3(2): 77
- Zhang K D, Wang W. *International Journal of Pressure Vessels and Piping*[J], 1987, 27(3): 223
- Kumar V, German M D. *Circumferential Through-wall Cracks*[J], 1988
- Zahoor A. *Circumferential Through-wall Cracks*[J], 1989
- Park J S, Choi Y H, Im S. *International Journal of Pressure Vessels and Piping*[J], 2014, 117-118(3): 17
- Kim Y J, Shim D J, Huh N S et al. *International Journal of Pressure Vessels and Piping*[J], 2002, 79(5): 321
- Kastner W, Röhrich E, Schmitt W et al. *International Journal of Pressure Vessels and Piping*[J], 1981, 9(3): 197
- Chen Xiangwei, He Xiaohua, Dai Qiao et al. *Rare Metal Materials and Engineering*[J], 2013, 42(7): 1469 (in Chinese)
- Dai Q, Zhou C Y, Peng J et al. *Rare Metal Materials and Engineering*[J], 2014, 43(2): 257
- Ren Jiatao, Chen Jiguang, Su Liwen et al. *Petro-Chemical Equipment*[J], 1998(6): 19 (in Chinese)
- Gan Weiping, Yang Zhiqiang, Wang Huimin. *Light Alloy Fabrication Technology*[J], 2002, 30(3): 43 (in Chinese)
- Bai Chenyang, Zhou Changyu, He Xiaohua et al. *Journal of Nanjing Tech University, Natural Science Edition*[J], 2016, 38(3): 38 (in Chinese)
- Dick C P, Korkolis Y P. *International Journal of Solids and Structures*[J], 2014, 51(18): 3042
- Guo Yanhong. *Thesis for Master*[D]. Nanjing: Nanjing Tech University, 2014 (in Chinese)
- Surh H B, Jang Y Y, Kim S C et al. *Theoretical and Applied Fracture Mechanics*[J], 2017, 30: 75
- Kim Y J, Huh N S, Kim Y J. *Engineering Fracture Mechanics*[J], 2002, 69(11): 1249
- Li Jian, Zhou Changyu. *Journal of Nan Jing Tech University, Natural Science Edition* [J], 2014, 36(6): 83 (in Chinese)
- Jeong J U, Choi J B, Kim M K et al. *International Journal of Pressure Vessels and Piping*[J], 2016, 146: 11

## 含环向穿透裂纹正交各向异性 TA2 管道的失效评定曲线

瞿文隽, 周昌玉, 于 勤

(南京工业大学, 江苏 南京 211816)

**摘要:** 运用三维有限元弹塑性分析计算了含环向穿透裂纹各向同性和正交各向异性 TA2 管道的极限载荷,  $J$  积分以及失效评定曲线。研究了不同几何尺寸和不同裂纹尺寸的管道以及正交各向异性对失效评定曲线的影响。结果表明: 正交各向异性管道与各向同性管道的极限载荷,  $J$  积分有明显差异。如果将正交各向异性材料视作各向同性, 当内压与极限载荷比  $L_r < 0.9$  时, 评定结果会比较保守, 相反当  $L_r > 0.9$  时, 评定结果会有一定的危险。对正交各向异性材料而言管道轴向力学性能强于环向时比较危险。因此对含环向穿透裂纹管道进行失效评定时, 材料正交各向异性的影响不能忽略。

**关键词:** TA2; 正交各向异性; 极限载荷;  $J$  积分; 失效评定曲线; 环向穿透裂纹管道

作者简介: 瞿文隽, 女, 1993 年生, 硕士生, 南京工业大学机械与动力工程学院, 江苏 南京 211816, 电话: 025-58139951, E-mail: 2435108315@qq.com